Research article

The mouse anterior chamber angle and trabecular meshwork develop without cell death

Richard S Smith[1,2], Adriana Zabaleta[2], Olga V Savinova[2] and Simon WM John*[1,2,3]

Address: [1]The Howard Hughes Medical Institute, [2]The Jackson Laboratory, 600 Main Street Bar Harbor, Maine and [3]The Department of Ophthalmology, Tufts University School of Medicine, Boston, Massachusetts

E-mail: Richard S Smith - rss@jax.org; Adriana Zabaleta - zabaleta@jax.org; Olga V Savinova - ovs@jax.org; Simon WM John* - swmj@jax.org
*Corresponding author

Published: 14 February 2001

BMC Developmental Biology 2001, 1:3

Received: 22 November 2000
Accepted: 14 February 2001

This article is available from: http://www.biomedcentral.com/1471-213X/1/3

Abstract

Background: The iridocorneal angle forms in the mammalian eye from undifferentiated mesenchyme between the root of the iris and cornea. A major component is the trabecular meshwork, consisting of extracellular matrix organized into a network of beams, covered in trabecular endothelial cells. Between the beams, channels lead to Schlemm's canal for the drainage of aqueous humor from the eye into the blood stream. Abnormal development of the iridocorneal angle that interferes with ocular fluid drainage can lead to glaucoma in humans. Little is known about the precise mechanisms underlying angle development. There are two main hypotheses. The first proposes that morphogenesis involves mainly cell differentiation, matrix deposition and assembly of the originally continuous mesenchymal mass into beams, channels and Schlemm's canal. The second, based primarily on rat studies, proposes that cell death and macrophages play an important role in forming channels and beams. Mice provide a potentially useful model to understand the origin and development of angle structures and how defective development leads to glaucoma. Few studies have assessed the normal structure and development of the mouse angle. We used light and electron microscopy and a cell death assay to define the sequence of events underlying formation of the angle structures in mice.

Results: The mouse angle structures and developmental sequence are similar to those in humans. Cell death was not detectable during the period of trabecular channel and beam formation.

Conclusions: These results support morphogenic mechanisms involving organization of cellular and extracellular matrix components without cell death or atrophy.

Background

Abnormal anterior segment development is often associated with elevated intraocular pressure (IOP), an important risk factor for the blinding disease glaucoma [1]. The anterior segment of the eye is filled with a clear fluid known as the aqueous humor or aqueous. Maintenance of IOP is dependent on a balance between aqueous formation and aqueous outflow. The primary source of aqueous is blood flowing through the arteries of the ciliary body [2]. The aqueous is secreted by the ciliary body

into the posterior chamber between the iris and lens. It then flows into the anterior chamber, the space between the cornea and iris, before draining from the eye at the iridocorneal junction [3]. The iridocorneal junction is located in a region known as the iridocorneal angle because of the aqueous filled angular recess between the iris root and cornea. One drainage route consists of a trabecular meshwork (TM) of connective tissue covered by endothelial like trabecular cells and a Schlemm's canal (SC). The aqueous percolates through channels or intertrabecular spaces in the TM before entering SC. The fluid collected by SC drains into aqueous veins that connect to the canal. This route is generally accepted to be the major drainage pathway for the aqueous [3]. Egress via the loose connective tissue meshwork and blood vessels of the uvea (choroid, iris and ciliary body) and the outer wall of the eye (sclera) also contributes to aqueous drainage [3, 4]. Primary access of aqueous to the uveoscleral route is likely deep in the angle recess at the iridocorneal junction. The resistance to aqueous flow presented by the tissues of the TM, SC, and likely uvea and sclera are important determinants of the rate of aqueous outflow and IOP.

The molecular mechanisms responsible for normal or abnormal development of the iridocorneal angle, its structures, and increased resistance to aqueous drainage in glaucoma are not well defined. Cell migration, proliferation, and differentiation are important for the development of this ocular region. Cells of the periocular mesenchyme migrate into the developing eye and differentiate into various anterior segment structures including components of the ciliary body, the TM, iris stroma, corneal endothelium and corneal stroma. The origin of the periocular mesenchyme was originally suggested to be the paraxial mesoderm [5]. Later fate mapping studies using quail-chick chimeras show extensive cranial neural crest contribution to this tissue [6, 7]. Based on these avian studies, the mammalian periocular mesenchyme is generally accepted as neural crest derived [8, 9]. Recent cell grafting and cell labeling studies of craniofacial morphogenesis in mouse embryos confirm a neural crest derivation of the mammalian periocular mesenchyme [10]. Additionally, however, they demonstrate the presence of cranial paraxial mesoderm-derived cells in this tissue. Thus, aberrations of both neural crest and mesoderm cell migration or differentiation may contribute to anterior segment dysgenesis and glaucoma.

After the migrating mesenchymal cells reach the anterior margin of the developing optic cup they must form the tissues of the iridocorneal angle. The iridocorneal angle is initially occupied by a densely packed mass of mesenchymal cells. As TM development proceeds the cellular mass differentiates, organizes and develops channels to produce the mature meshwork. The developing TM and iris separate forming the deep angle recess through which the aqueous passes to access the TM. The mature meshwork consists of trabecular beams separated by intertrabecular spaces through which the aqueous percolates. The trabecular beams are covered on both surfaces by endothelial-like trabecular cells and the cores of the beams are composed of extracellular matrix components such as collagen and elastic tissue [11].

How the complex TM develops and how spaces form in the initially continuous cellular tissue is not clear. Several theories have attempted to explain the differentiation and morphogenesis of the mesenchyme that forms the tissues of the iridocorneal angle (see [12,13 ,14,15,16 ,17]). Some of these theories propose atrophy or resorption of the mesenchyme as development progresses to create the structures and spaces important for aqueous drainage while others propose a reorganization of cells with no cell death or atrophy. Whether cell death or atrophy occurs during TM and iridocorneal angle development remains controversial. Cell death was prominent in rat, but not in monkey, human or dog eyes [17,18,19, 20,21]. It is not clear if different mechanisms are important in rodents as compared to these other species, if there is something unusual about the studied rat strain, or if cell death occurs in the other species but was not detected due to inadequate tissue sampling or the stages analyzed.

The mouse represents an important experimental model for understanding mammalian development and diseases caused by its abnormalities. In studied mammalian species, iridocorneal angle development is incomplete at birth. Although various studies have characterized in detail the prenatal development of the mouse eye there is very little published about the normal structure or postnatal development of the mouse iridocorneal angle [22 ,23,24,25 ,26,27]. The aims of this work were to determine the developmental profile of the mouse iridocorneal angle to its mature form and to assess the role of cell death in modeling the angle recess and TM. We present a light and electron microscopic (EM) evaluation of iridocorneal angle development in staged embryos and through eight postnatal weeks, when the angle structures have reached full maturity. The mouse and human TM and SC have similar structures, and the developmental progression is similar except for the accelerated time frame in mice. Extensive use of light microscopy, EM and a cell death assay (on sections spanning complete eyes) failed to identify cell death at all tested ages in various mouse strains. These results substantiate models of iridocorneal angle mesenchymal differentiation and modeling that involve organization of

cellular and extracellular matrix components without cell death or atrophy, and they suggest a conservation of developmental mechanisms between mice and non-rodent mammals.

Results

The following descriptions reflect the most common situation at a specific time as determined from the analysis of multiple animals and sections of different locations around the eyes. Important developmental stages are summarized in Figure 1. Figure 2B to 2D shows important changes during embryonic development. Figure 2E to 2I and Figure 3A to 3D show postnatal development. Figure 3E to 3H shows the mature angle structure in four different strains.

Prenatal development

This study of the prenatal development of the C57BL/6J iridocorneal angle, essentially agrees with published reports of general ocular development for the strains CFI-S [24] and Ha/1CR [22]. Due to these previous reports, we will focus on the formation of the iridocorneal angle structures (see figure 2A for location) with brief mention of the adjacent iris and cornea. Invagination of the optic vesicle to form the optic cup occurs around E10, as the lens vesicle is developing [22]. Shortly after the stalk of the lens vesicle disappears at E10.5, a few undifferentiated mesenchymal cells were present adjacent to the anterior margin of the optic cup. These were more prominent by E11.5 and were associated with blood vessels (Figure 2B) that become the source of the anterior vascular tunic of the lens as well as contributing to the future vascular supply of the iris and ciliary body. At this time, progenitor cells of the corneal stroma had migrated into the developing cornea (not shown). By E14.5, the anterior margin of the optic cup that ultimately forms the iris and ciliary body has started to advance indicating that the anterior uvea and iridocorneal angle were starting to form. The mesenchyme in the developing iridocorneal angle (angle mesenchyme) had produced a loosely arranged cluster of cells that was several cells thick and extended from the anterior edge of the optic cup to the anterior termination of the retina. These cells were characterized by plump oval nuclei with multiple nucleoli. There was no clear division between the mesenchyme of the posterior corneal surface and the angle mesenchyme because the cells remained undifferentiated (Figure 2C). By E16.5 the anterior margin of the optic cup had extended more anteriorly but no obvious differentiation into the iris and ciliary body had occurred. The angle mesenchyme was more densely packed and continuous with the mesenchyme extending onto the primitive iris that will become the iris stroma (Figure 2D). There was a clear separation between the developing iris and cornea, the first appearance of the iridocorneal angle recess (Figure 2D). There were no obvious differences between E16.5 and E18.5 except that the ciliary body had started to form as previously reported [22].

Postnatal development

At birth (P0, 19.5 dpc), the angle mesenchyme was even more densely packed and the cells and their nuclei were more elongated and less rounded than at earlier stages (Figure 2E). The iris was more differentiated as evidenced by the fact that some of the cells destined to form the stroma had started to synthesize pigment and were, therefore, distinguishable from those of the future TM. The iris and ciliary body became separate as the ciliary processes continued to form (Figure 2E).

The specialized basal lamina of the corneal endothelium (Descemet's membrane) was first evident at P2 to P4. By P4, the iris and ciliary body were well developed. Pigmented cells and blood vessels were clearly evident in the iris stroma and the ciliary processes were elongated and more numerous (Figure 2F). The future location of the TM was clearly indicated by an aggregation of cells with densely stained, plump fusiform nuclei that separated the developing ciliary body from the cornea (Figure 2F).

The angle mesenchyme extended from the termination of Descemet's membrane to the posterior termination of the ciliary body by P8. These cells were less densely packed than at earlier stages (Figure 2G). Although not definitively identified in our P8 sections, at some locations there appeared to be small vascular channels present near the developing TM. The ciliary processes and iris had an apparently mature structure by P10. By this age, the anterior cells of the future TM had begun to separate, although the posterior cells remained closely packed (Figure 2H). The first clear indications of Schlemm's canal next to the developing TM were observed on P10 as multiple small endothelial-lined channels located in the inner sclera over the posterior aspect of the ciliary body, although this was best seen using transmission EM (see below). The presence or absence of these endothelial channels at this location varied with ocular region. The anterior TM had started to separate focally from the iris at P10, and this was more extensive at P12. The angle mesenchyme had further developed into beam like structures by P12 and, though small, more open spaces were apparent (Figure 2I). At P12 either endothelial-lined vessels or a more mature SC were present in most sections.

By P14, further spaces had opened in the angle, especially anteriorly, and for the first time there was a consistent separation between the anterior TM and iris root, forming the deep angle recess (Figure 3A). At this age, a SC that extended from the posterior end of the ciliary body

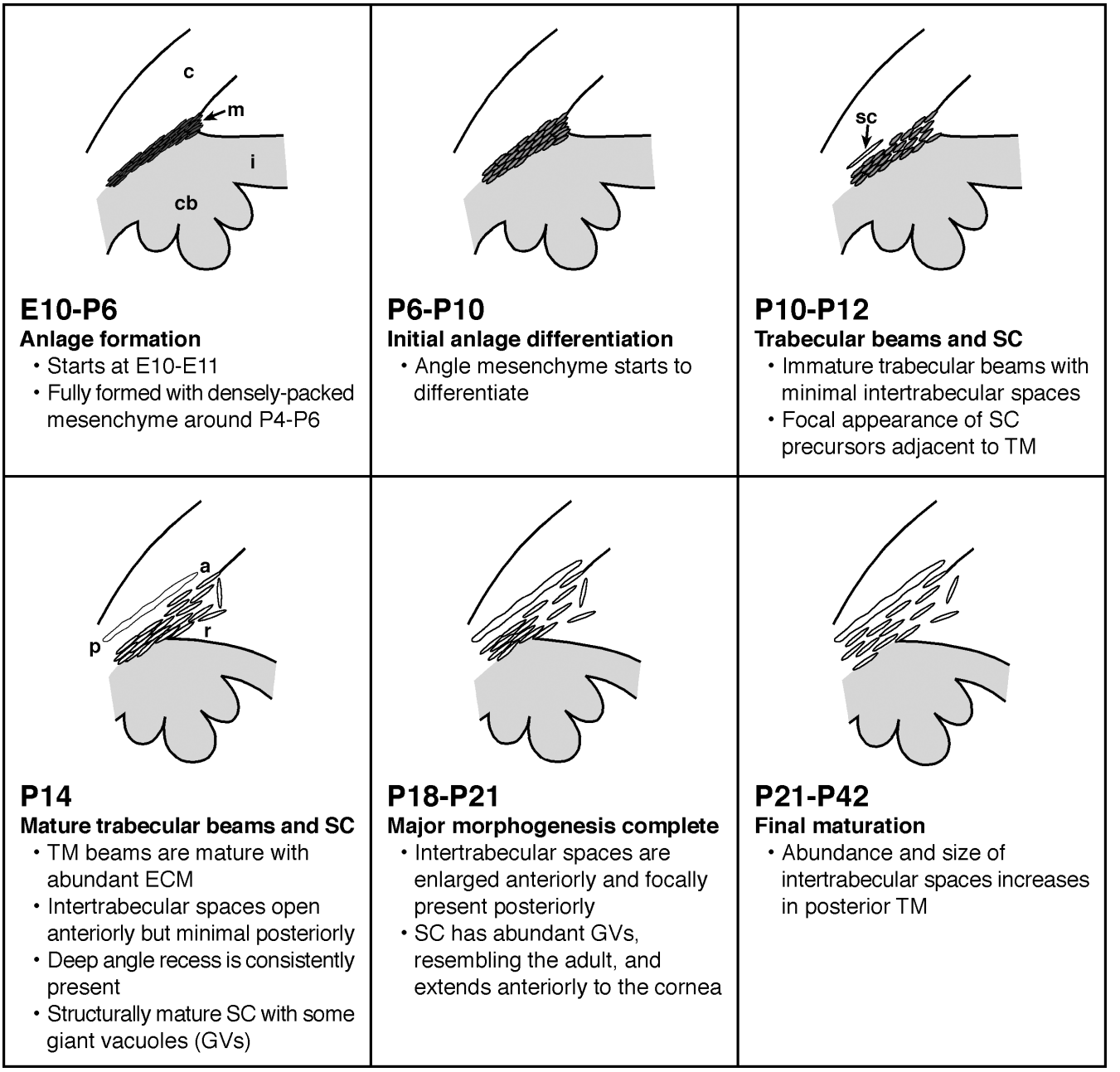

Figure 1
Formation of the mouse iridocorneal angle. A diagrammatic representation of iridocorneal angle morphogenesis is shown. c = cornea, cb = ciliary body, i = iris, m = angle mesenchyme, sc = Schlemm's canal, r = deep angle recess. a = anterior, p = posterior.

to a point slightly posterior to the end of Descemet's membrane was consistently observed in all ocular regions. Additionally, the separation of the iris away from the TM gave the appearance that SC and TM moved anteriorly. Giant vacuoles (structures important for aqueous movement from the TM to canal lumen) were clearly observed indicating that SC was functional at P14 (Figure 3A). By three weeks of age, SC had extended forward to the posterior termination of Descemet's membrane and large open spaces were present in the anterior TM. Fewer spaces were evident in the posterior TM (Figure 3B). Over the next few weeks, the spaces between the trabecular beams gradually became more open and extended further into the posterior TM. Depending on the mouse and ocular location, the iridocorneal angle and its structures typically reached their mature state by P35 to P42

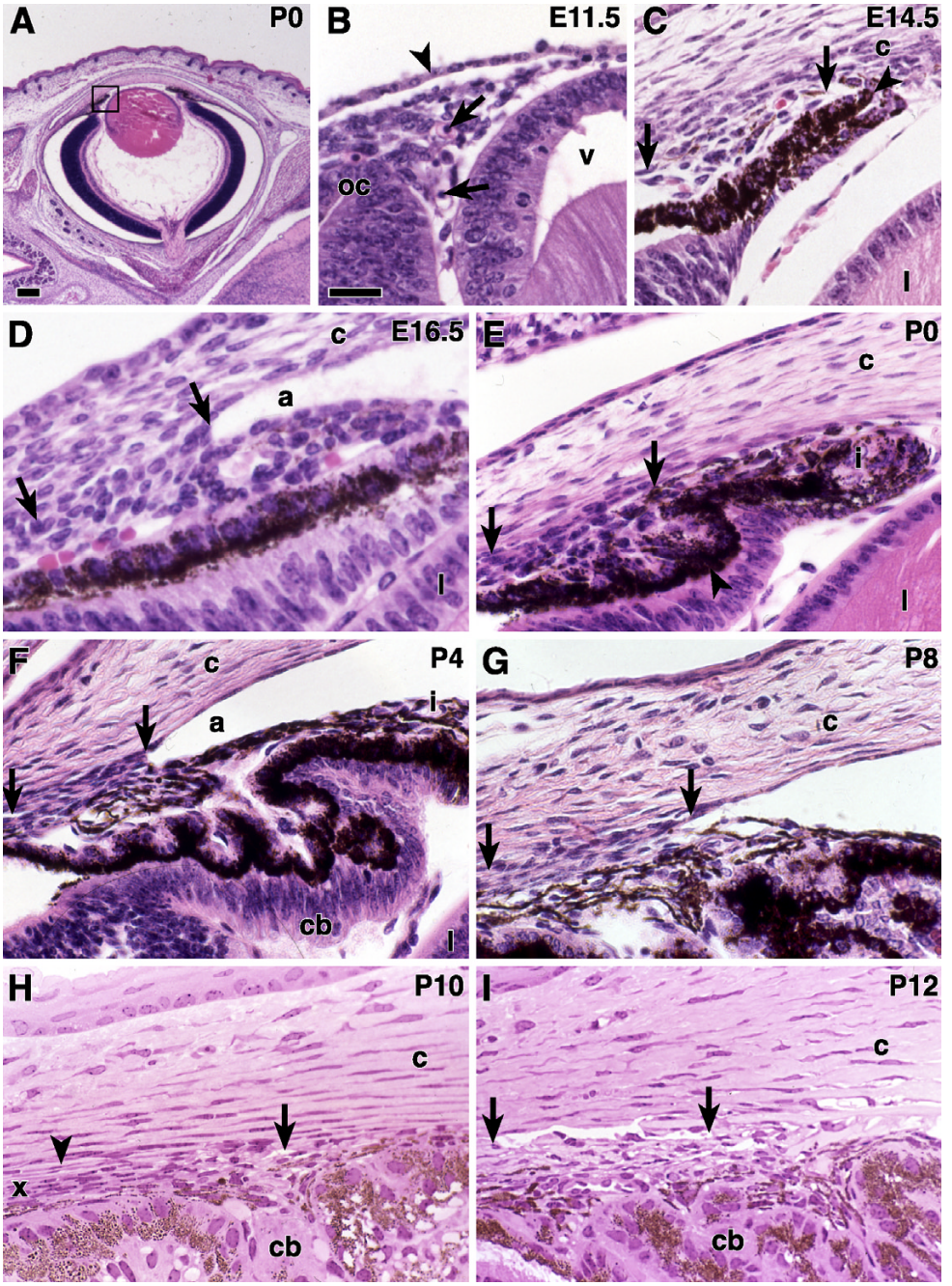

Figure 2
Iridocorneal angle E11.5 to P12 Images from paraffin (**A** -**G**) and plastic (**G**-**H**) embedded B6 eyes of the indicated ages. (**A**) The box indicates the iridocorneal angle region that is illustrated at high power in the other panels of Figures 1 and 2. (**B**) At E11.5, loose mesenchymal tissue is present between the anterior edge of the optic cup (oc), the lens vesicle (v), and the surface ectoderm (arrowhead). Primitive vascular channels contain nucleated red blood cells (arrows). (**C**) At E14.5, two layers of epithelium form the OC region that will develop into the iris and ciliary body. The anterior layer is heavily pigmented (arrowhead). The arrows indicate the anterior and posterior extent of undifferentiated angle mesenchyme. The cornea (c) and lens (l) are well defined. (**D**) At E16.5, a small angle recess is present (a). The location of the future TM is evident (arrows). (**E**) In a newborn mouse, the mesenchyme of the developing iris (i) and TM (arrows) regions are distinguishable. The TM cells have elongated, more densely-staining nuclei and are arranged in lamellae (arrows). The ciliary processes (arrowheads) have begun to form. The angle recess is artifactually compressed in this image. (**F**) At P4, there is a long angle recess (a), and the iris and ciliary body (cb) are well formed. The cells of the future TM (arrows) show a dense lamellar arrangement. (**G**) At P8, the developing TM is less compressed than at earlier ages (arrows). (**H**) At P10, an endothelial lined vascular channel (arrowhead) is present at some locations. Intertrabecular spaces have begun to open in the anterior portion of the TM (arrow). The posterior aspect of the TM remains compressed (x). (**I**) At P12, A well-formed SC (arrows) is easily identified exterior to the posterior TM. Internal to SC, both anterior and posterior meshwork has become more open. Bars 200 μm (**A**) and 40 μm (**B-I**).

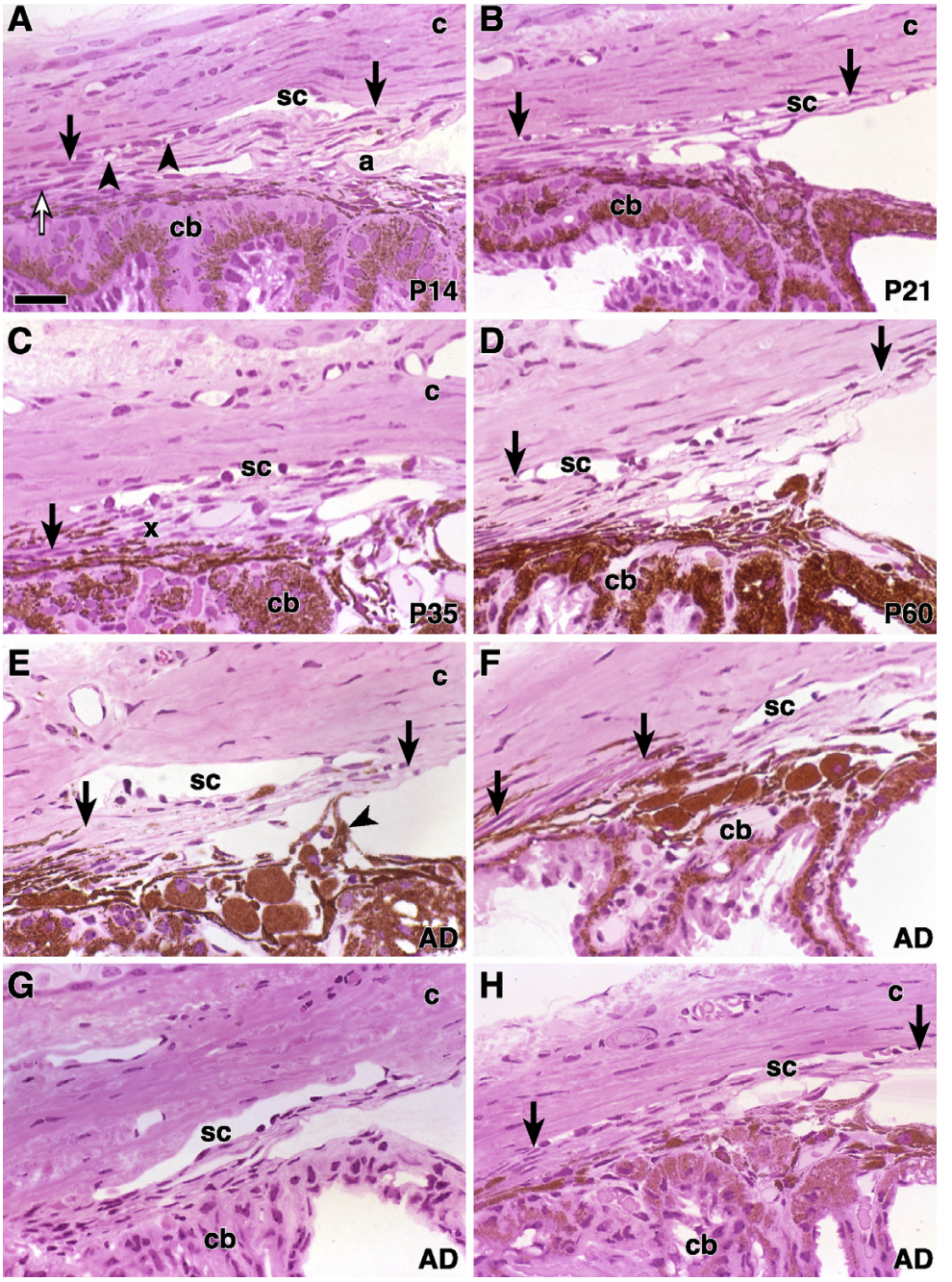

Figure 3
Iridocorneal angle P14 to P63 Hematoxylin and eosin stained plastic sections from mice of the indicated ages. (**A-D**) strain B6. (**A**) At P14, SC (arrows) contains vacuolar structures (arrowheads) that were confirmed to be giant vacuoles by EM (see below). The developing ciliary muscle is characterized by eosinophilic cytoplasm (open arrow). Intertrabecular spaces are obvious in the anterior TM and the deep angle recess (a) is present as a space between the anterior TM and iris root. c = cornea, cb = ciliary body. (**B**) By P21, SC (arrows) extends from the posterior ciliary body to the end of Descemet's membrane. There are large spaces in the anterior TM. (**C**) By P35 there is further opening of the intertrabecular spaces that extend more posteriorly. The posterior TM (x) remains closely attached to the ciliary body, as it does in the adult. The ciliary muscle (arrow) consists of a few muscle fibers. (**D**) This P60 eye has a well developed SC (arrows) and TM and is very similar to that shown for P35. Comparison to older mice (up to 1 year old, not shown) indicates that the iridocorneal angle has reached maturity. The adult structure is similar in other mouse strains (**E-H**). All of the adult mice were approximately 63 days old. (**E**) A 129/SvEvTac mouse has a robust TM (arrows) and a broad SC. An iris process attaches to the anterior TM (arrowhead). (**F**) In this 129BS mouse, there is a robust TM and SC. The ciliary muscle (arrows) is particularly prominent in this strain. (**G**) BALB/cByJ. (**H**) In this DBA/2J mouse, SC is present but shows mild artifactual compression (arrows). Bar 40 μm.

(compare Figure 3C and 3D). In the mature state, the intertrabecular spaces were always most prominent in the anterior aspect of the TM, and less so posteriorly (Figure 3C and 3D).

Other strains

The postnatal developmental stages and time frame described above for B6 mice is essentially the same as that we observed for the A.BY/SnJ strain (not shown). There were no major differences in mature angle structure between mice of different backgrounds, and the anterior to posterior TM differences described for B6 were evident in all strains (Figure 3E-3H). The biggest difference between the studied backgrounds was a consistently more robust ciliary muscle in the 129BS mice.

Electron microscopy

To further understand iridocorneal angle development, we analyzed stages involving significant changes in the TM and SC using EM. Ultrastructural evaluation demonstrated that differentiation of the TM was well underway by P10. Trabecular beams were recognizable but not fully developed. The separation of individual trabecular beams had begun and extracellular matrix deposition was evident. While present, trabecular beam collagen was less abundant than in the mature eye, while elastic tissue was relatively more abundant (compare Figure 4D and 4E to Figure 5F and 5G). The trabecular beams were more separated in the anterior than posterior TM. The presence of SC or its precursors varied with section level at P10. At some locations there were no traces of SC (Figure 4A) whereas at others it was relatively well formed with a thin endothelial lining (Figure 4B). No giant vacuoles were observed at this age. At other levels of section, the early SC had a more primitive vascular appearance (Figure 4C), consistent with its likely derivation from coalescing venules.

At P14, spaces between the trabecular beams in the anterior TM were typically more prominent than at P10. The posterior TM remained relatively compressed compared to the anterior TM, with smaller intertrabecular spaces (Figure 5A, 5B). The extracellular matrix was more prominent than at P10 (compare Figure 5A to Figure 4A). A well developed, endothelial-lined SC was consistently present at all levels (Figure 5B), although giant vacuoles were relatively infrequent compared to older ages. By P18, the intertrabecular spaces had enlarged to adult size even in some regions of the posterior TM and giant vacuoles were abundant (Figure 5C). Smooth muscle cells (Figure 5D) located near the inner wall of SC close to its posterior termination were first noted at P14. The major developmental changes had occurred by P18, with subsequent maturation primarily involving final enlargement of spaces in the posterior TM.

In adult mice, SC was lined with attenuated endothelial cells and at low power several giant vacuoles were always present (Figure 5E). Giant vacuoles were evenly distributed along the entire length of Schlemm's canal. There were 3-4 trabecular beams in the anterior meshwork and 7-10 in the posterior meshwork. In the posterior adult meshwork, the extracellular matrix was more prominent and the intertrabecular spaces were smaller than anteriorly (Figure 5F, 5G).

Absence of cell death in angle development

Review of many sections examined by light microscopy did not identify dead or pyknotic cells at any age from PO to adult. Similar review of many sections by EM failed to demonstrate any cells that had necrotic or apoptotic morphology. This was true for multiple mouse strains (see Methods). It is probable that all normal cell death during development utilizes pathways of programmed cell death (PCD) [28]. To further investigate if cell death occurred in the developing iridocorneal angle, we used a fluorescent double labeling assay that identifies fragmented DNA using fluorescently labeled dUTP and detects chromatin condensation by binding of the dye YOYO-1. Cells were identified as apoptotic only when they were doubly labeled (Figure 6). This assay is more sensitive than light microscopy and allows more widespread testing than EM. As shown above, TM channel formation has started at P10 and is mostly complete around P18 to P20, with subtle changes extending to P35 to P42. Our assay investigated tissues that spanned most of this period (see Methods), including four time points in the critical period surrounding P10 to P18 (P10, P12, P14 and P18). The majority of the angle was assessed by analyzing many sections that were obtained at 20 μm intervals throughout the eye. During differentiation from the trabecular anlage to a mature state, only 2 doubly labeled cells were identified in the angles of approximately 600 analyzed sections or approximately 120,000 analyzed TM and SC cells. One of these positive cells was located in the lumen of Schlemm's canal and was likely a blood cell. No apoptotic cells were detected in the ciliary body and iris. In contrast, apoptotic retinal ganglion cells (Figure 6) were frequently identified (often 2 or more apoptotic cells in a section) during the established period of developmental ganglion cell death (assessed between P10 and P21) and less abundantly afterwards. Testis sections served as additional positive controls with each batch of processed slides, and abundant apoptotic cells were always detected.

As a final assessment of a role for cell death pathways, we determined whether absence of the FAS and FASL initiators of cell death alter iridocorneal angle development and morphology. *Fas* and *FasL* are expressed in the TM and a FAS-stimulating monoclonal antibody causes PCD

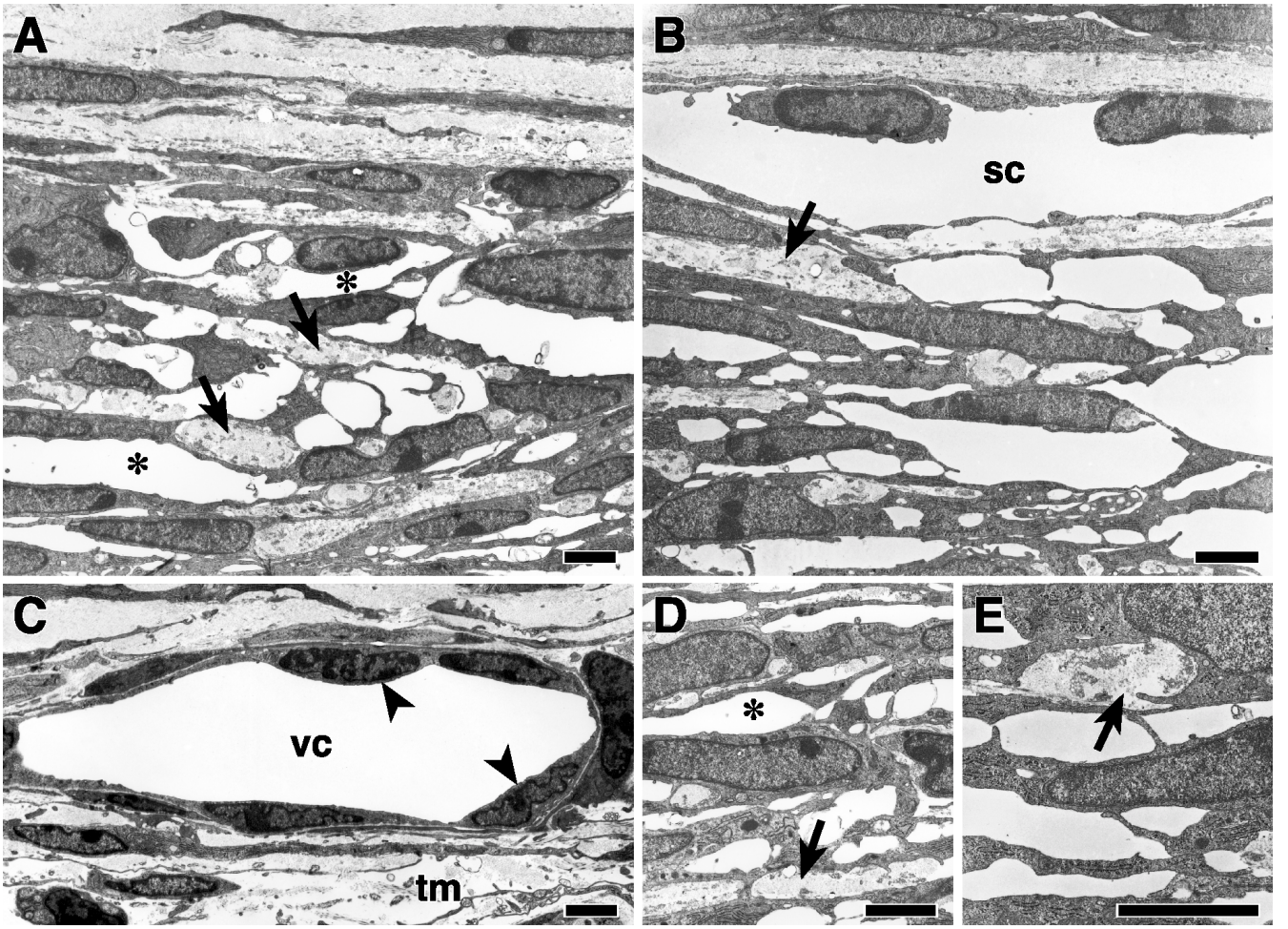

Figure 4
Ultrastructure of the TM and SC in B6 mice at P10 (**A, D**) In the posterior TM, spaces are developing between the trabecular beams (asterisks). Small amounts of collagen and elastic tissue are demonstrated within the beams (arrows). Schlemm's canal is absent in these sections. (**B, E**) In the anterior TM, the spaces between adjacent trabecular beams are generally larger than posteriorly (compare B and E that are anterior to A and D that are posterior). SC is present in **B** but giant vacuoles are absent. Elastic tissue and collagen (arrows) are present in amounts similar to that of the posterior meshwork. (**C**) In a different level of section to **B**, SC is represented by a vascular channel (vc) adjacent to the differentiating TM (tm). The endothelial cells (arrowheads) lining this channel are less attenuated than in the adult SC and giant vacuoles are absent. Bars 1 μm.

of TM cells [29, 30]. We assessed five mice of each of the mutant strains B6.MRL-*Fas* ^{lpr} and B6Smn.C3H-*Fasl* ^{gld}, which respectively lack functional FAS and FASL. The eyes of mice lacking functional FAS or FASL were similar in appearance to eyes from age-matched B6 mice (not shown). This indicates that these pro-apoptotic molecules are not required for normal iridocorneal angle development.

Discussion

Sequence and timing of iridocorneal angle morphogenesis

In this study, we describe the morphogenesis of the mouse iridocorneal angle from prenatal stages to maturity. Our findings extend those of previous studies that did not focus on the iridocorneal angle or did not study its development to maturity [22,23,24,25,26]. The sequence and timing of morphogenic events in the C57BL/6J and A.BY/SnJ mouse strains is summarized in Figure 1, and is similar to that for rats [31]. The sequence also is similar in humans. The major difference is the age at which specific developmental stages occur, beginning prenatally but extending to around P42 in mice and possibly to 8 postnatal years in humans [16, 19].

Briefly, in mice, migrating mesenchyme begins to fill the space between the anterior edge of the optic cup, the surface ectoderm and the lens vesicle at E11 to E12. Anlage formation appears complete by P4 to P6. Cell differenti-

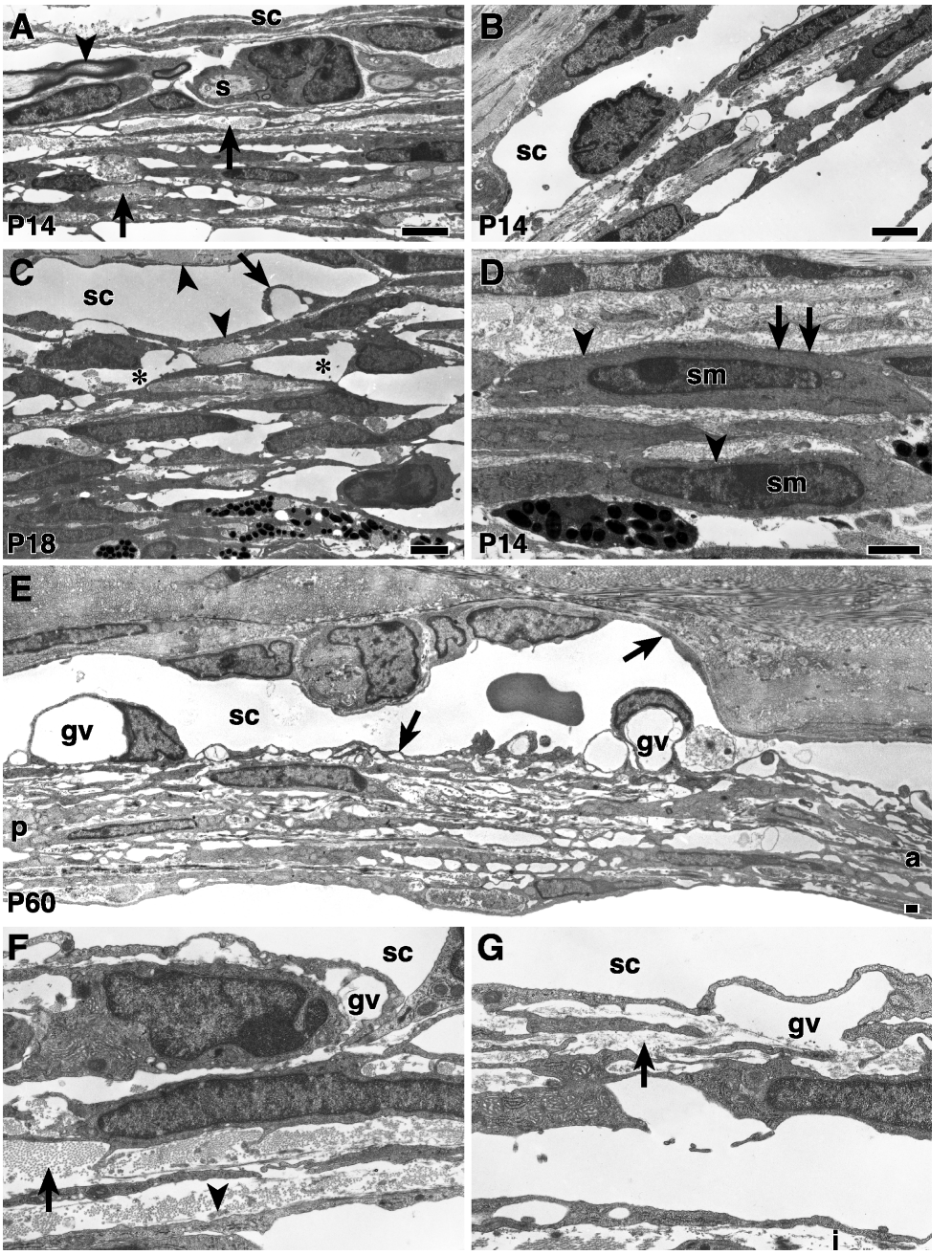

Figure 5

Ultrastructure of the TM and SC in B6 mice from P14 to P60 (**A**, **B**, **D**) are from the same P14 mouse. (**A**) At P14 the spaces in the posterior TM are smaller than at older ages (compare to a P18 eye in **C**). Trabecular beam collagen and elastic tissue (arrows) is more abundant than at younger ages. A Schwann cell (s) and accompanying myelinated nerve (arrowhead) are present close to SC. (**B**) In the anterior TM, there is a well-developed SC, but giant vacuoles are not common. There are fewer trabecular beams and larger intertrabecular spaces than in the posterior TM (compare to **A,** and see **F, G**). (**C**) The spaces (asterisks) between trabecular beams in this region of the posterior TM are more extensive than at P14. SC is lined by a thin endothelium (arrowheads) and contains giant vacuoles (arrow). (**D**) Smooth muscle cells (sm) lie internal to Schlemm's canal near its posterior termination. They are characterized by pinocytotic vesicles near the cell membrane (arrowheads), focal density of the plasma membrane (arrows) and cytoplasmic filaments (not seen at this magnification). (**E**) At P60, SC is lined by attenuated endothelium (arrows) and contains giant vacuoles (gv). a = anterior, p = posterior. (**F**) Partial segment of the posterior TM at P60. The trabecular beam extracellular matrix is dense. Collagen (arrow) is abundant while elastic tissue (arrowhead) is relatively sparse. (**G**) In the anterior TM, the beams are more delicate, and contain less extracellular matrix (arrow). A portion of the anterior iris (i) is present in this image. Bars 1 μm.

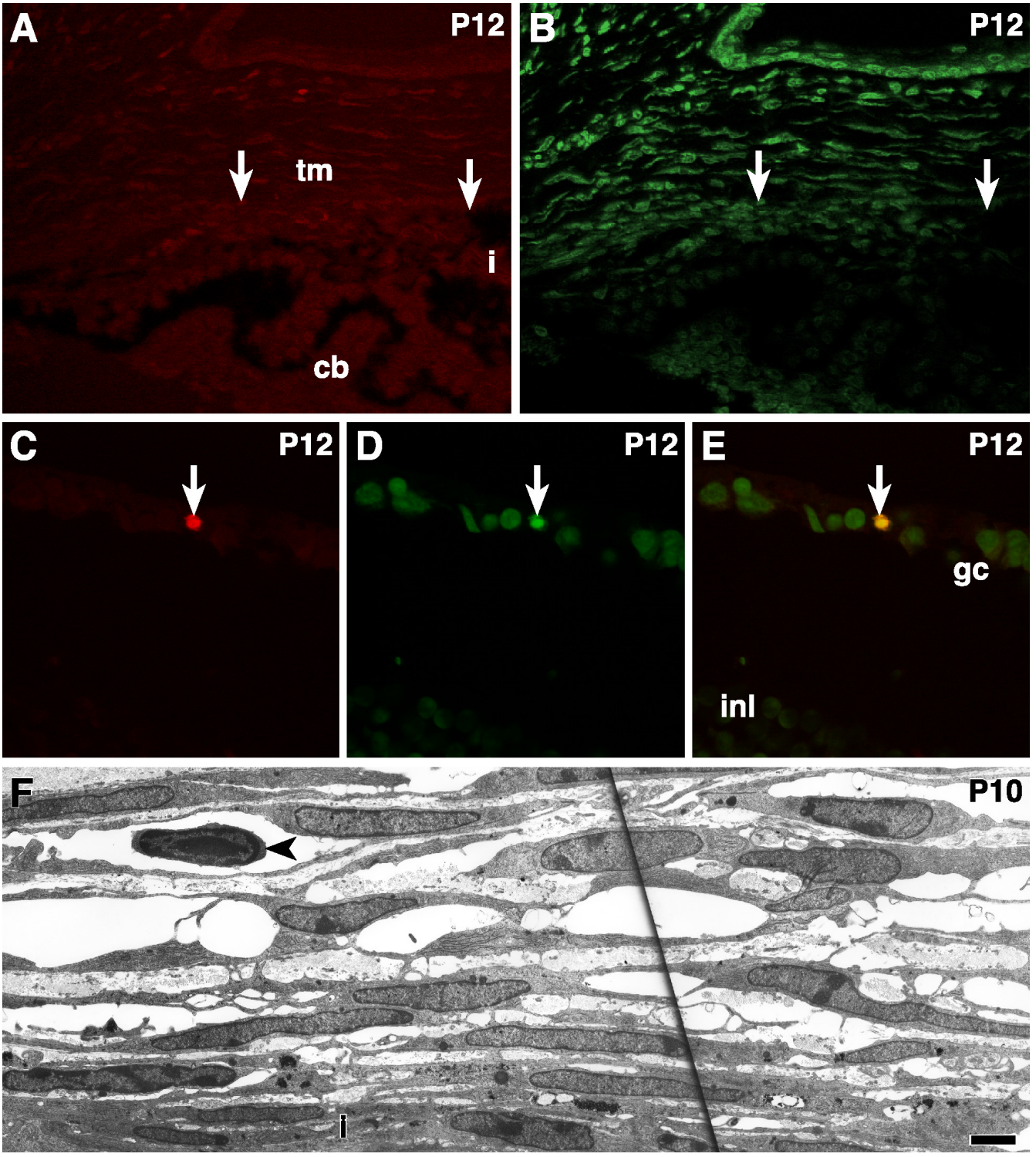

Figure 6

Absence of cell death in the developing iridocorneal angle. A double labeling assay that identifies fragmented DNA using fluorescently labeled dUTP (**A**, **C**) and detects chromatin condensation by binding of the dye YOYO-1 (**B**, **D**) was used to detect programmed cell death (PCD). Both assays were negative in a P12, B6 iridocorneal angle (**A**, **B**). The same was true for many sections at ages that spanned angle morphogenesis. i= iris, cb = ciliary body, arrows indicate the extremities of the TM (tm). (**C, D, E**) A cell undergoing PCD (arrow) is identified by double labeling in the retinal ganglion cell layer (gc) of the same eye shown in **A** and **B.** inl = inner nuclear layer. Dying retinal ganglion cells (RGCs) acted as internal positive controls for the PCD assays. Testis sections served as additional positive controls with each batch of processed slides, and abundant apoptotic cells were always detected. (**F**) Morphologic features of cell death were absent in the TM of a P10, B6 mouse. The trabecular cells demonstrate normal nuclei and normal cytoplasmic morphology. The same was true in many sections of eyes of different ages and strains. The iris (i) is resting against the inner edge of this central portion of the TM. A small lymphocyte (arrowhead) lies in the space between two trabecular beams. Bar 1 μm.

ation within the anlage has started by P8. Trabecular beams are recognizable but not fully developed at P10. SC is first evident around P10 and appears structurally mature around P14. Although SC is functional at this age, giant vacuoles are rare. By P18 to P21, the major developmental changes have occurred, and intertrabecular spaces have enlarged to adult size in the anterior TM and some parts of the posterior TM. Giant vacuoles become more abundant as spaces between the trabecular beams increase and are abundant at P18 to P21. After P18-P21, maturation primarily involves enlargement of spaces in the posterior TM.

Participation of cell death in iridocorneal angle morphogenesis is controversial

Different theories on the mechanisms of morphogenesis of the angle mesenchyme to the complex tissues of the mature angle have been reviewed elsewhere [12,13, 14,15,16, 17]. Important mechanisms that participate in complex tissue formation include: proliferation and differentiation of cells, differential growth rates of cells, modulation of the extracellular matrix, and cell death. Although there is evidence for a role of most of these processes in iridocorneal angle development and intertrabecular space opening (see [17]), the role of cell death or atrophy is controversial.

In Sprague Dawley (SD) rats, dying cells were readily identified from P5 to P100 (average of 10 to 20 dying cells per section) and less abundantly at older adult ages (1 to 3 per section at P200) [18]. This time frame encompasses the period of mesenchymal differentiation and channel formation in the rat angle (P5 to P60). Due to this and the fact that dying cells were identified in the TM, iris, iris root and ciliary body, it was proposed that cell death may serve to open the deep angle recess and to create spaces in the TM and uveoscleral outflow routes. The dying cells were frequently associated with macrophages. An established function of macrophages is the engulfment of cellular debris. Macrophages also can elicit cell death in normal development (see [32]). In the developing eye, macrophages are required to induce death of vascular endothelial cells during programmed capillary regression. Disruption of macrophage function prevents endothelial cell death and results in abnormal persistence of the capillary networks known as the pupillary membrane and hyaloid vasculature [33, 34]. Together, these observations suggest that macrophage induced cell death may be important in angle morphogenesis.

By contrast to the rat study, trabecular cell death was not observed or was rare in the developing human, monkey and dog TM [12, 16, 17, 20 , 21], even though small numbers of macrophages were present in some of these studies. In one human study that considered total cell numbers (as opposed to cell density), the total number of cells increased as the TM matured. Macrophages were reported in the developing mouse (B6) anterior chamber and a model of TM development including cell death was proposed, but no cell death was recorded [26]. The reason for these differing results is still unclear, and may reflect factors such as the age of tissue sampled or the amount of tissue available for study.

No evidence for cell death during mouse angle development

We report here an extensive study of mouse eyes. Light microscopy failed to detect cell death in the developing TM of B6 and A.BY/SnJ mice. Dying cells were not detected in the angle of mice of an additional 5 inbred strains and 3 mixed genetic backgrounds at ages up to P63. No cells with the characteristic morphologic changes of apoptosis or necrosis were observed by EM [35, 36] in mice of strain B6, or of 5 other inbred strains and 2 mixed genetic backgrounds at ages up to P63. Similarly, only 2 apoptotic cells were detected in the developing SC, TM, iris and ciliary body of B6 eyes using a cell death assay on sections collected throughout entire eyes. In contrast, apoptotic cells were frequently identified in the developing retinas on the same sections. Importantly, the great majority of TM channel formation occurs during an 8 to 10 day period surrounding P10 to P18. Our EM and fluorescent PCD assays included three (P10, P14 and P18) and four (P10, P12, P14 and P18) time points respectively during this critical period. Although rare cases of cell death may be missed, the absence of cell death in approximately 600 analyzed sections provides no evidence for a role of cell death in angle morphogenesis. Finally, development of the angle in *Fas* and *Fasl* null mice was normal indicating this system of cell death regulators that can kill TM cells [30] is not required for TM channel formation. Based on these observations, we conclude that neither apoptosis nor necrosis are important mechanisms in development of the mouse TM and iridocorneal angle. Our data, together with the rare occurrence of cell death in studies of various mammalian species including humans, suggests that this is true for mammals in general.

Possible explanations for conflicting results between various studies

The absence of macrophages in the developing TM of mice in the current study is in conflict to a previous study. That study reported macrophages on the corneal endothelium, on the iris surface and in the TM at P6 through P10 [26]. The abundance of TM macrophages was not reported but the statement that they were observed in "favorable sections" suggests that they were not common. Macrophage mediated regression of the

pupillary membrane occurs between P4 and P10 in mice [33, 37]. In the current investigation, we observed macrophages in the anterior chamber between the iris and cornea, and associated with the pupillary membrane between P6 and P10. Thus, we suggest that the macrophages previously reported in TM of mice (and possibly some other species) were involved in the process of pupillary membrane regression and were sometimes deposited in the TM but were not significant for TM development. That TM cell death was not recorded in both studies supports this.

The demonstration of cell death in a SD strain of rats has fueled the debate about mechanisms of iridocorneal angle development [18]. This report disagrees with our findings in mice and warrants further discussion. In this rat strain, conspicuous numbers of macrophages were noted associated with dying cells in the iris, ciliary body and TM. Given the similarities in developmental stages between both B6 and A.BY/SnJ mouse strains and humans, and the similar timing and progression of angle development in mice and rats, it seems unlikely that mechanisms of angle morphogenesis would differ between mice and rats. It is, therefore, difficult to reconcile the frequent cell death in the developing and adult iridocorneal angle of an SD rat strain with the absence of cell death in multiple mouse strains in the current study. Although structural features and not morphogenesis were the focus of other rat studies, cell death was not reported in an EM analysis of the adult TM of Swiss albino rats, or of the adult angle of an unspecified strain of pigmented lab rats [38, 39]. These findings suggest that the SD rat strain may have atypical or excessive intraocular macrophage recruitment, formation, stimulation or persistence that may explain the macrophage abundance and cell death. Spontaneous axonal regeneration was recently reported in the transected optic nerve of adult SD rats [40]. This was unexpected because, in contrast to peripheral nerves, axons of the adult, mammalian central nervous system typically fail to regenerate following injury. Regeneration is a complex and poorly understood process in which macrophages are known to be important. Addition of appropriately stimulated macrophages can induce a peripheral nerve-like regenerative response in the damaged rat optic nerve [41 ,42,43]. Although the spontaneous axonal regeneration in SD rats is consistent with atypical macrophage activity, further experiments are needed to test this.

Conclusions

Our results support a model of mesenchymal differentiation and iridocorneal angle development that involves reorganization of cellular and extracellular matrix components without cell death or atrophy. The use of genetically different mouse strains indicates that the absence of cell death is typical in mice and not unique to an individual strain. The lack of cell death, similar developmental profile, and similarities in mature angle structure in both humans and mice suggests a conservation of general developmental mechanisms between mice and non-rodent mammals. For general anterior segment development, this is supported by the observations that genetic deficiency of transcription factors such as PAX6, PITX2, FOXC1 [44,45], and LMX1B that are expressed in the periocular mesenchyme results in anterior segment dysgenesis in both humans and mice [46,47,48, 49,50,51,52,53,54]. In general, however, previous mouse studies have not examined the effects of mutations on the TM and SC. This is partly due to limited documentation of the sequence of events underlying iridocorneal angle development and limited documentation of the mature angle structures in mice. The current study provides important baseline information for mechanistic studies of angle development in the existing mouse models of anterior segment dysgenesis. Additionally, it will facilitate experiments with mutant mice to determine how newly identified genes function in angle development and how the pathways in which they participate overlap or interact with each other. These experiments will enhance understanding of the developmental processes involved in anterior segment formation, and glaucomas associated with anterior segment dysgenesis.

Materials and Methods

All experiments were performed in compliance with the ARVO statement for use of animals in vision research.

Light microscopy

At least three mice C57BL/6J (B6) were evaluated for each postnatal time period: newborn, P2, 4, 6, 8, 10, 12, 14, 21, 28, 35, 42, 49, and P56. Adult B6 mice ranging from P60 to 12 months and prenatal B6 stages E10.5 to E18.5 were also examined. Additionally, progressive developmental stages in the strain A.BY/SnJ were evaluated (P1, 7, 14, 21, 28, 35 42, and P60, with 2 to 6 mice at each age). A.BY/SnJ were normal mice derived from the A.BY/SnJ-*corn1* strain. At least 2 mice (7 to 9 weeks old) were used for each of the following strains or mixed backgrounds: DBA/2J, BALB/cByJ, 129P3/J (former name 129/J), 129SvEvTac, 129SvB6F2, 129P3B6F1 and 129BS (129SvEvTac X Black Swiss >F2). Four week old DBA/2J and SB/Le mice also were studied. To determine if absence of the cell death mediators FAS and FASL alter iridocorneal angle development and morphology, we assessed five mice (approximately P70) of each of the mutant strains B6.MRL-*Fas* ^{lpr} and B6Smn.C3H-*Fasl* ^{gld}, which respectively lack functional FAS and FASL [55,56,57,58].

For stages E11.5 through P6, whole heads were fixed in Bouin's solution, paraffin embedded and sectioned at 5 μm thickness. Eyes from mice of ages P8 and older were fixed with a glutaraldehyde-paraformaldehyde solution [53], plastic embedded, sectioned at 1.5 μm thickness and stained with hematoxylin and eosin. For both paraffin and plastic-embedded B6 eyes, 25 to 40 sections were collected from each of 3 different ocular locations, using the lens as a landmark, resulting in 75 to 120 sections per eye. Collected regions included the lens periphery, central lens, and a region halfway between the center of the lens and the lens periphery. Iridocorneal angle development is somewhat variable both temporally and spatially within a single eye and between eyes. This necessitated careful scanning of all sections. The eyes of other strains were processed identically, except that 30 to 40 sections through the pupil and optic nerve were typically collected and analyzed. This also was true for some of the adult eyes from B6 mice that were P60 or older. Developmental changes had to be consistently present in multiple sections from the same region to be regarded as real, and conclusions were drawn only from high quality sections. This approach guarded against the potential for distortion artifacts in the delicate tissues analyzed.

Electron microscopy

To assess developmental stages and to check for cell death, we studied eyes from three or more B6 mice at P10, 14, 18, 21, 35, and P60; from 2 DBA/2J and 2 SB/LE mice at 4 weeks of age; and from at least two 7 to 9 week old DBA/2J, BALB/cJ, 129P3/J, 129SvEvTac, 129B6F1 and 129BS mice. Eyes were processed as previously described [53]. Tissue blocks from 6 to 8 different locations around the eye were sectioned and analyzed for each eye.

Fluorescent programmed cell death (PCD) assays

B6 eyes at P10, 12, 14, 18, 21, 29 and P36, were immediately fixed in 4% paraformaldehyde in 0.1 M phosphate buffer pH 7.2 for 3 hours, transferred to 0.4% paraformaldehyde in 0.1 M phosphate buffer for 48 hrs, and infiltrated with paraffin. Eyes from two different mice in each age group were sectioned at 5 μm thickness and sections were collected at 20 μm intervals through the entire eye, except for very peripheral locations that did not contain iridocorneal angle. Depending on the size of the eye between 30 and 81 sections were collected per eye. We analyzed approximately 600 sections and estimate that considering all ages there was on average 100 cells in each angle region of our sections. Thus, we analyzed approximately 120,000 developing TM and SC cells (100 cells X 600 sections X 2 angle regions per section). A modified double labeling protocol that involved *in situ* end-labeling of fragmented DNA (using BODIPY fluorophores, Molecular Probes, Eugene, Or.) and detection of condensed chromatin (with the dimeric cyanine dye YOYO-1, Molecular Probes) was used to analyze all of these sections [59]. Samples were analyzed with a confocal microscope and cells were identified as apoptotic only when they were double labeled. The occurrence of PCD was evaluated in the iris, ciliary body and TM.

Acknowledgments

We thank Janice Martin and Carol Ficket for animal husbandry; Lesley Bechtold; Priscilla Jewett and other members of The Jackson Laboratory Scientific Services for technical assistance; Felicia Farley for help with references; Jennifer Smith for help with figures; Joseph Cohen for support, and members of the John Lab, Thomas Gridley, Timothy O'Brien and Barbara Knowles for critical reading of the manuscript. We are also grateful to Nadine Tatton and William Tatton for their assistance with the fluorescent PCD assays and Alexander Chervonsky for the *Lpr* and *Gld* mice. Supported in part by CORE grant CA34196. SWMJ is an Assistant Investigator of The Howard Hughes Medical Institute.

References

1. Ritch R, Shields MB, Krupin T: **The Glaucomas, Clinical Science, 2nd edn.** *St. Louis, MO: Mosby-Year Book;* 1996,
2. Caprioli J: **The ciliary epithelia and aqueous humor.** *In: Adler's Physiology of the Eye Edited by William M. Hart J, 9th ed. pp. 228-247. St. Louis: Mosby Year Book;* 1992, 228-247
3. Hart WM: **Intraocular Pressure.** *In: Adler's Physiology of the Eye Edited by William M. Hart J, 9th ed. pp. 248-267. St. Louis: Mosby Year Book;* 1992, 248-267
4. Bill A: **Uveoscleral drainage of aqueous humor: physiology and pharmacology.** *Prog Clin Biol Res* 1989, **312**:417-427
5. Mann IC: **The Development of the Human Eye, First edn.** *Cambridge: Cambridge University Press;* 1928,
6. Johnston MC, Noden DM, Hazelton RD, Coulombre JL, Coulombre AJ: **Origins of avian ocular and periocular tissues.** *Exp. Eye Res.* 1979, **29**:27-43
7. Noden DM: **Periocular mesenchyme: neural crest and mesodermal interations.** *In: Ocular anatomy, Embryology and Teratology Edited by Jakobiec FA. pp. 97-119. Hagerstown, MD: Harper & Row;* 1982, 97-119
8. Kupfer C, Kaiser-Kupfer MI: **New hypothesis of developmental anomalies of the anterior chamber associated with glaucoma.** *Trans. Ophthalmol. Soc. U. K.* 1978, **98**:213-215
9. Tripathi BJ, Tripathi RC: **Neural crest origin of human trabecular meshwork and its implications for the pathogenesis of glaucoma.** *Am. J. Ophthalmol.* 1989, **107**:583-590
10. Trainor PA, Tam PP: **Cranial paraxial mesoderm and neural crest cells of the mouse embryo: co-distribution in the craniofacial mesenchyme but distinct segregation in branchial arches.** *Development* 1995, **121**:2569-2582
11. Gong H, Tripathi RC, Tripathi BJ: **Morphology of the aqueous outflow pathway.** *Microsc. Res. Tech.* 1996, **33**:336-367
12. Wulle KG: **The development of the productive and draining system of the aqueous humour in the human eye.** *Adv. Ophthalmol.* 1972, **26**:269-355
13. Tripathi BJ, Tripathi RC, Wisdom JE: **Embryology of the Anterior Segment of the Human Eye.** *In: The Glaucomas Edited by Ritch R, Shields MB, Krupin T, vol. 1, Second ed. pp. 3-38. St. Louis, MO: Mosby Year Book;* 1996, 3-38
14. deLuise VP, Anderson DR: **Primary infantile glaucoma (congenital glaucoma).** *Surv. Ophthalmol.* 1983, **28**:1-19
15. McMenamin PG: **Human fetal iridocorneal angle: a light and scanning electron microscopic study.** *Br. J. Ophthalmol.* 1989, **73**:871-879
16. McMenamin PG: **A morphological study of the inner surface of the anterior chamber angle in pre and postnatal human eyes.** *Curr. Eye Res.* 1989, **8**:727-739
17. McMenamin PG: **A quantitative study of the prenatal development of the aqueous outflow system in the human eye.** *Exp. Eye Res.* 1991, **53**:507-517
18. Reme C, Urner U, Aeberhard B: **The occurrence of cell death during the remodelling of the chamber angle recess in the**

developing rat eye. *Graefes Arch Clin Exp Ophthalmol* 1983, **221**:113-121
19. Reme C, d'Epinay SL: **Periods of development of the normal human chamber angle.** *Doc. Ophthalmol.* 1981, **51**:241-268
20. Smelser GK, Ozanics V: **The development of the trabecular meshwork in primate eyes.** *Am. J. Ophthalmol.* 1971, **71 Suppl**:366-385
21. Samuelson DA, Gelatt KN: **Aqueous outflow in the beagle. I. Postnatal morphologic development of the iridocorneal angle: pectinate ligament and uveal trabecular meshwork.** *Curr. Eye Res.* 1984, **3**:783-794
22. Pei YF, Rhodin JA: **The prenatal development of the mouse eye.** *Anat. Rec.* 1970, **168**:105-125
23. Kaufman MH: **The Atlas of Mouse Development.** *San Diego: Academic Press;* 1995,
24. Rugh R: **Organogeny.** *In: The Mouse Its Reproduction and Development. pp. 208-295. Minneapolis: Burgress Publishing Co.;* 1968, 208-295
25. Vanden Hoek TL, Goossens W, Knepper PA: **Fluorescence-labeled lectins, glycoconjugates, and the development of the mouse AOP.** *Invest. Ophthalmol. Vis. Sci.* 1987, **28**:451-458
26. Beauchamp GR, Lubeck D, Knepper PA: **Glycoconjugates, cellular differentiation, and congenital glaucoma.** *J. Pediatr. Ophthalmol. Strabismus.* 1985, **22**:149-155
27. Cook CS, Sulik KK: **Sequential scanning electron microscopic analyses of normal and spontaneously occurring abnormal ocular development in C57BL/6J mice.** *Scan. Electron Microsc.* 1986, **3**:1215-1227
28. Jacobson MD, Weil M, Raff MC: **Programmed cell death in animal development.** *Cell* 1997, **88**:347-354
29. Griffith TS, Brunner T, Fletcher SM, Green DR, Ferguson TA: **Fas ligand-induced apoptosis as a mechanism of immune privilege.** *Science* 1995, **270**:1189-1192
30. Agarwal R, Talati M, Lambert W, Clark AF, Wilson SE, Agarwal N, Wordinger RJ: **Fas-activated apoptosis and apoptosis mediators in human trabecular meshwork cells.** *Exp. Eye Res.* 1999, **68**:583-590
31. Reme C, Urner U, Aeberhard B: **The development of the chamber angle in the rat eye. Morphological characteristics of developmental stages.** *Graefes. Arch. Clin. Exp. Ophthalmol.* 1983, **220**:139-153
32. Lang R, Lustig M, Francois F, Sellinger M, Plesken H: **Apoptosis during macrophage-dependent ocular tissue remodelling.** *Development* 1994, **120**:3395-3403
33. Lang RA, Bishop JM: **Macrophages are required for cell death and tissue remodeling in the developing mouse eye.** *Cell* 1993, **74**:453-462
34. Diez Roux G, Lang RA: **Macrophages induce apoptosis in normal cells in vivo.** *Development* 1997, **124**:3633-3638
35. Kerr JF, Wyllie AH, Currie AR: **Apoptosis: a basic biological phenomenon with wide-ranging implications in tissue kinetics.** *Br. J. Cancer* 1972, **26**:239-257
36. Wyllie AH: **Cell Death: A new classification separating apoptosis from necrosis.** *In: Cell Death in Biology and Pathology Edited by Bowen ID, Lockshin RA. pp. 9-29. London: Chapman & Hall;* 1981, 9-29
37. Ito M, Yoshioka M: **Regression of the hyaloid vessels and pupillary membrane of the mouse.** *Anat. Embryol. Berl.* 1999, **200**:403-411
38. McMenamin PG, Al-Shakarchi MJ: **The effect of various levels of intraocular pressure on the rat aqueous outflow system.** *J Anat* 1989, **162**:67-82
39. van der Zypen E: **Experimental morphological study on structure and function of the filtration angel of the rat eye.** *Ophthalmologica* 1977, **174**:285-298
40. Campbell G, Holt JK, Shotton HR, Anderson PN, Bavetta S, Lieberman AR: **Spontaneous axonal regeneration after optic nerve injury in adult rat.** *Neuroreport* 1999, **10**:3955-3960
41. Perry VH, Brown MC: **Role of macrophages in peripheral nerve degeneration and repair.** *Bioessays* 1992, **14**:401-406
42. Lazarov Spiegler O, Solomon AS, Schwartz M: **Peripheral nerve-stimulated macrophages simulate a peripheral nerve-like regenerative response in rat transected optic nerve.** *Glia* 1998, **24**:329-337
43. Lazarov Spiegler O, Solomon AS, Schwartz M: **Link between optic nerve regrowth failure and macrophage stimulation in mammals.** *Vision Res.* 1999, **39**:169-175
44. Nishimura DY, Swiderski RE, Alward WLM, Searby CC, Patil , Benner SR, Kanis AB, Gastier JM, Stone EM, Sheffield VC: **The folkhead transcription factor gene FKHL7 is responsible for glaucoma phenotypes which map to 6p25.** *Nat. Genet.* 1998, **19**:140-147
45. Mears AJ, Jordan T, Mirzayans F, Dubois S, Kume , Parlee M, Ritch R, Koop B, Kuo WL, Collins C, Marshall J, Gould DB, Pearce W, Carlsson P, Enerback S, Morissette J, Bhattacharya S, Hogan B, Raymond V, Walter MA: **Mutations of the forkhead/winged-helix gene, FKHL7, in patients with Axenfeld-Rieger anomaly.** *AM. J. Hum. Genet.* 1998, **63**:1316-1328
46. Hill RE, Favor J, Hogan BL, Ton CC, Saunders GF, Hanson IM, Prosser J, Jordan T, Hastie ND, van Heyningen V: **Mouse small eye results from mutations in a paired-like homeobox-containing gene.** *Nature* 1991, **354**:522-525
47. Hanson IM, Fletcher JM, Jordan T, Brown A, Taylor D, Adams RJ, Punnett HH, van Heyningen V: **Mutations at the PAX6 locus are found in heterogeneous anterior segment malformations including Peters' anomaly.** *Nat. Genet.* 1994, **6**:168-173
48. Semina EV, Reiter R, Leysens NJ, Alward WL, Small KW, Datson NA, Siegel Bartelt J, Bierke Nelson D, Bitoun P, Zabel BU, Carey JC, Murray JC: **Cloning and characterization of a novel bicoid-related homeobox transcription factor gene, RIEG, involved in Rieger syndrome** *Nat. Genet.* 1996, **14**:392-399
49. Pressman CL, Chen H, Johnson RL: **Lmx1b, a LIM homeodomain class transcription factor is necessary for normal development of multiple tissues in the anterior segment of the murine eye.** *Genesis* 2000, **26**:15-25
50. Gage PJ, Suh H, Camper SA: **Dosage requirement of Pitx2 for development of multiple organs.** *Development* 1999, **126**:4643-4651
51. Kidson SH, Kume T, Deng KY, Winfrey V, Hogan BLM: **The forkhead/winged-helix gene, Mf1, is necessary for the normal development of the cornea and formation of the anterior chamber in the mouse eye.** *Dev. Biol.* 1999, **211**:306-322
52. Kume T, Deng KY, Winfrey V, Gould DB, Walter MA, Hogan BL: **The forkhead/winged helix gene Mf1 is disrupted in the pleiotropic mouse mutation congenital hydrocephalus.** *Cell* 1998, **93**:985-996
53. Smith RS, Zabaleta A, Kume T, Savinova OV, Kidson SH, Martin JE, Nishimura DY, Alward WLM, Hogan BLM, John SWM: **Haploinsufficiency of the transcription factors FOXC1 and FOXC2 results in aberrant ocular development.** *Hum. Mol. Genet.* 2000, **9**:1021-1032
54. Lichter PR, Richards JE, Downs CA, Stringham HM, Boehnke M, Farley FA: **Cosegregation of open-angle glaucoma and the nail-patella syndrome.** *Am. J. Ophthalmol.* 1997, **124**:506-515
55. Nagata S, Golstein P: **The fas death factor.** *Science* 1995, **267**:1449-1456
56. Vercammen D, Brouckaert G, Denecker G, Van de Craen M, Declercq W, Fiers W, Vandenabeele P: **Dual signaling of the Fas receptor: initiation of both apoptotic and necrotic cell death pathways.** *J. Exp. Med.* 1998, **188**:919-930
57. Watanabe Fukunaga R, Brannan CI, Copeland NG, Jenkins NA, Nagata S: **Lymphoproliferation disorder in mice explained by defects in Fas antigen that mediates apoptosis.** *Nature* 1992, **356**:314-317
58. Lynch DH, Watson ML, Alderson MR, Baum PR, Miller RE, Tough T, Gibson M, Davis Smith T, Smith CA, Hunter K, *et al*: **The mouse Fas-ligand gene is mutated in gld mice and is part of a TNF family gene cluster.** *Immunity* 1994, **1**:131-136
59. Tatton NA, Maclean Fraser A, Tatton WG, Perl DP, Olanow CW: **A fluorescent double-labeling method to detect and confirm apoptotic nuclei in Parkinson's disease.** *Ann. Neurol.* 1998, **44**:S142-S148